Polymer Journal (2013) 45, 269–276

www.nature.com/pj

FOCUS REVIEW

Bio-inspired synthesis of polymer–inorganic nanocomposite materials in mild aqueous systems

Ayae Sugawara-Narutaki

It is increasingly important that we learn how to fabricate materials in environmentally friendly ways using common resources that are abundant in nature. Biomineralization, the process by which living organisms create a variety of sophisticated composites, such as bone and shell, is an ideal model for such fabrication. This article reviews recent progress toward the synthesis of polymer–inorganic composite materials inspired by biomineralization. In particular, three reaction systems are focused upon: (1) polymer–calcium carbonate thin film composites synthesized by interaction among insoluble polymer, soluble acidic polymer, and inorganic ions, (2) polymer nanogel–calcium phosphate composite nanoparticles synthesized on scaffolds of hydrogel nanoparticles and (3) colloidal silica nanoparticles made to self-assemble into anisotropic chain-like structures by interaction with block copolymers. All these reaction systems involve aqueous environments at ambient temperature and pressure.
Polymer Journal (2013) **45,** 269–276; doi:10.1038/pj.2012.171; published online 19 September 2012

Keywords: biomineralization; calcium carbonate; calcium phosphate; polymer–inorganic composite; self-assembly; silica

INTRODUCTION

Materials fabrication in an environmentally friendly, energy-efficient manner is an urgent imperative in today's society. Nature's ingenious methods of materials synthesis, wherein living organisms create a variety of sophisticated bio-architectures in water-based systems at ambient temperature and pressure, is an ideal model to pursue. Biominerals, such as seashells, bone, coccoliths, and diatoms, are excellent examples of bio-architectures.[1–5] Seashell nacre has a brick-and-mortar structure of plate-like calcium carbonate ($CaCO_3$) and thin sheets of protein–polysaccharide matrix.[4] In addition, bone has a hierarchical structure of oriented crystals of calcium phosphate and collagen fibrils.[5]

The key to biomineralization processes is the interaction among organic molecules, polymers and inorganic ions, which unite into highly organized hybrid bio-architectures.[1–5] Although the overall process of biomineralization is too complicated to mimic in its entirety, materials scientists can learn the molecular-control approach as the essence of the process, and integrate it with modern technology.[1,3,6–8] In this manuscript, three of the bio-inspired approaches to the construction of nanostructured polymer–inorganic composite materials in mild aqueous systems are reviewed.

POLYMER–$CaCO_3$ THIN FILM COMPOSITE MATERIALS

$CaCO_3$ is one of the most abundant minerals on earth. Many living organisms use $CaCO_3$ for protection in the form of shells or exoskeletons. Seashell nacre is a particularly well-designed biomineral.[4] Nacre is formed by crystallization of $CaCO_3$ in the preformed compartments of an insoluble matrix (chitin/silk fibroin-like proteins) in the presence of water-soluble acidic proteins (Figures 1a and b). $CaCO_3$ nucleation and crystal growth are finely controlled by the interaction between calcium ions and organic components, and results in the formation of plate-like $CaCO_3$ crystals with controlled polymorph and crystallographic orientation. The plate-like $CaCO_3$ crystals are composed of bridged nanocrystals that have a similar orientation.[9] The cooperative involvement of insoluble and soluble macromolecules during crystallization of inorganic compounds seems to be a general strategy in biomineralization.[1]

Nacre formation was mimicked by Kato *et al.*[10–14] to synthesize polymer–$CaCO_3$ thin film composites. The combination of an insoluble solid matrix with soluble acidic macromolecules induces thin film crystallization of $CaCO_3$ on the matrix (Figures 1c and d). For the insoluble solid matrix, the researchers chose chitin, chitosan and cellulose, which contain functional groups such as OH and NH moieties. For the soluble acidic macromolecules, they chose poly (acrylic acid) (PAA), poly(glutamic acid) (PGlu) and poly(aspartic acid) (PAsp). A supersaturated solution of $CaCO_3$ was prepared by dissolving $CaCO_3$ powder in water while carbon dioxide (CO_2) gas was introduced. A solid matrix was prepared by spin coating the polymer solution on a glass substrate. The matrix was then immersed in a supersaturated solution of $CaCO_3$ ($[Ca^{2+}] \sim 8$ mM, 30 °C) containing soluble polymer. Slow release of CO_2 from the solution accompanied precipitation of $CaCO_3$ according to the following equation:

$$Ca^{2+}(aq) + 2HCO_3^-(aq) \rightleftarrows CaCO_3(s) + CO_2(g) + H_2O \quad (1)$$

Department of Chemical System Engineering, School of Engineering, The University of Tokyo, Tokyo, Japan
Correspondence: Dr A Sugawara-Narutaki, Department of Chemical System Engineering, School of Engineering, The University of Tokyo, 7-3-1 Hongo, Bunkyo-ku, Tokyo 113-8656, Japan.
E-mail: ayae@chemsys.t.u-tokyo.ac.jp
Received 28 July 2012; revised 4 August 2012; accepted 6 August 2012; published online 19 September 2012

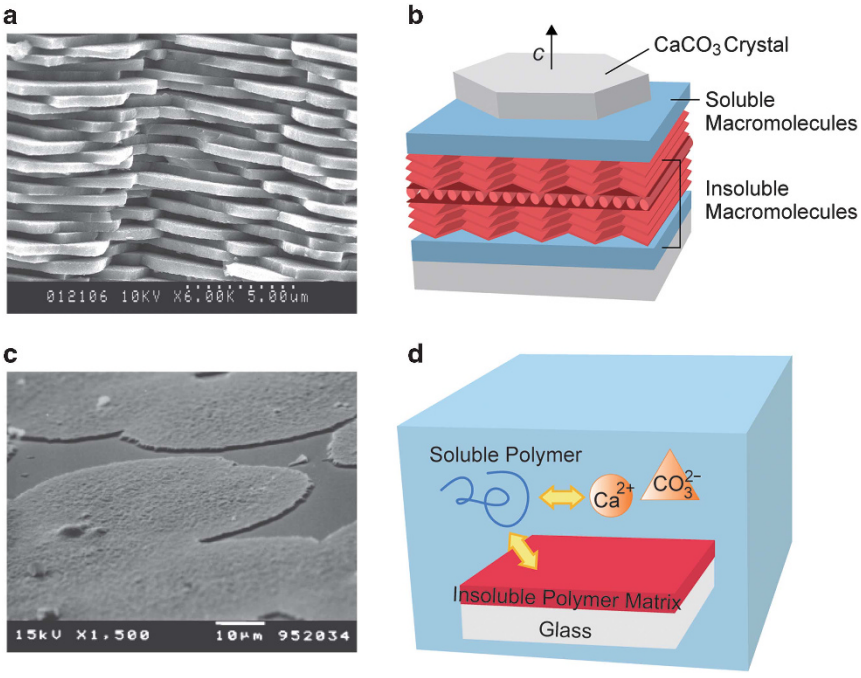

Figure 1 (**a**) Scanning electron microscopy (SEM) image of the fractured nacre of abalone. (**b**) Schematic illustration of the composite structure of nacre. (**c**) SEM image of thin film crystals of $CaCO_3$ formed on a chitin matrix in the presence of PAA. Reprinted with permission from Kato *et al.*[13] Copyright (2000), The Chemical Society of Japan. (**d**) Schematic illustration of the experimental setup for preparing $CaCO_3$ thin films.

$CaCO_3$ crystallization began at multiple nucleation sites on the matrix surface, and by 20 h it had spread over the entire matrix. The resulting $CaCO_3$ film, <1-μm thick, was composed of nanocrystals about 10–20 nm in size.[15] Significantly, only a small amount of soluble polymer was needed to achieve thin film crystallization; for example, PAA gave a $CaCO_3$ thin film on a chitosan matrix at concentrations in the range from 2.4×10^{-4} to 1.0×10^{-2} wt%.[14] The likely mechanism of this thin film formation is as follows: the polysaccharide OH and NH moieties interact with the acidic macromolecule carboxylates in solution and results in adsorption of the macromolecules onto the matrix surface. The macromolecules then bind calcium ions to result in a high local concentration of calcium ions on the matrix surface, which induces nucleation of $CaCO_3$. Homogeneous nucleation of $CaCO_3$ in solution is inhibited by the acidic polymers dissolved in the crystallization medium. On the basis of these findings by Kato *et al.*, a variety of $CaCO_3$/polymer composites with controlled structures are prepared as described below.

$CaCO_3$ thin films with controlled polymorphs

$CaCO_3$ has three crystalline polymorphs: calcite, aragonite and vaterite. Of these, thermodynamically, calcite is most stable and vaterite is least stable. An amorphous form of $CaCO_3$ (ACC) also exists. Polymorph control of $CaCO_3$ is a significant aspect of biomineralization. For example, a mollusk shell's nacre consists of aragonite, whereas its outer layer consists of calcite. ACC is stabilized in the exoskeleton of crustaceans. As each polymorph has different physical properties, organisms employ the most suitable polymorph for the required purpose. Polymorph control of $CaCO_3$ during fabrication of $CaCO_3$-containing composite materials is also important from the viewpoint of materials science. Accordingly, aragonite $CaCO_3$ thin films on solid matrices that resemble partial lamellar sheets of nacre have been prepared by the following two methods.

The first method of aragonite thin film preparation exploits the known capability of magnesium ion (Mg^{2+}) to facilitate aragonite formation by inhibiting the crystal growth of other polymorphs.[16,17] For $CaCO_3$ crystallization under ambient conditions, aragonite is the kinetically favored precipitate from solutions with [Mg]/[Ca] ratios of $\geqslant 4$.[16] The question of whether the effect of Mg^{2+} is compatible in a polymer-mediated $CaCO_3$ crystallization system has been examined. Aragonite thin films have been successfully formed on a chitosan matrix in the presence of PAsp and $MgCl_2$.[18] The fraction of aragonite increases with increasing $[Mg^{2+}]/[Ca^{2+}]$ ratio,[19] with essentially pure aragonite film obtained at $[Mg^{2+}]/[Ca^{2+}] = 6$ (Figure 2a). A $CaCO_3$ thin film composed of a mixture of calcite, aragonite and vaterite is deposited without the presence of $MgCl_2$ (Figure 2b). The rate of crystal growth is twice as slow in the presence of Mg^{2+} as in its absence; it takes about 40 h for aragonite films to fully cover the chitosan surface because this method exploits the inhibition effect of calcite and vaterite.

The second method of thin film preparation exploits the fact that aragonite thin films can be obtained using the template effect of polymers without the presence of Mg^{2+}. Crystalline poly(vinyl alcohol) (PVA) has a suitable structure for this purpose, with the distance between its hydroxyl groups almost equal to the distance between calcium ions in aragonite's *ab* plane. Crystalline PVA matrix has been obtained by annealing PVA film at 200 °C for 30 min. An aragonite thin film has been formed on PVA matrix with the aid of PAA.[20] It is speculated that PAA adsorbed on crystalline PVA can partially form aligned carboxylic acid moieties because PAA and PVA have common main-chain structures. The aligned and partially deprotonated COOH groups might act as templates for aragonite formation by interacting with Ca^{2+}. Interestingly, vaterite forms

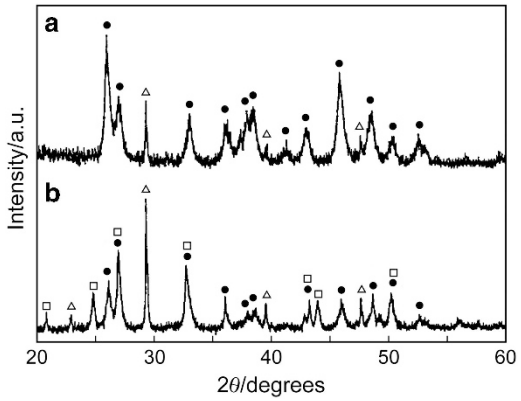

Figure 2 X-Ray diffraction patterns of $CaCO_3$ thin films grown on chitosan matrices in the presence of PAsp: (**a**) in the presence of $MgCl_2$ ($[Mg^{2+}]/[Ca^{2+}] = 6$) and (**b**) in the absence of $MgCl_2$; aragonite (●), calcite (Δ) and vaterite (□). Adapted with permission from Sugawara *et al.*[18] Copyright (2000), Royal Society of Chemistry.

when PGlu is used instead of PAA. PGlu may not provide aligned COOH groups due to a mismatch in the backbone structures of PGlu and PVA.

$CaCO_3$ thin film composite with patterned structure

Morphological control for $CaCO_3$ films has been achieved using a soft-gel matrix as a thin solid matrix.[21–24] The hydrophobized polysaccharide cholesterol-bearing pullulan (CHP) has been used as a soft-gel matrix for $CaCO_3$ crystallization (Figure 3a).[21,22] Akiyoshi *et al.*[25] reported that CHPs form hydrogels in water due to association of the cholesteryl groups, which function as physical crosslinking points. CHP matrix was immersed in calcium chloride solution ($[Ca^{2+}] = 10$ mM, 20 °C) containing PAA (2.4×10^{-3} wt%). Crystallization was induced by diffusion of ammonium carbonate vapor into calcium chloride solution for 2 days. Surprisingly, calcite films with periodic surface-relief structures formed on the CHP matrix in the presence of PAA (Figures 3b and c).[21,22] As such relief structures function as diffraction gratings, the calcite film appears iridescent in color under irradiation with white light. It is assumed that this periodic pattern formation is a result of self-organization in reaction–diffusion systems where competition between precipitation and ion diffusion exists. Indeed, such behavior is usually observed in gel media. This assumption is consistent with the fact that pattern formation is greatly influenced by temperature (which affects the rate of both crystal growth and ion diffusion) and by the substitution degree of cholesterol in CHP that is needed to alter the crosslinking degree of the matrix (which affects the rate of ion diffusion).

PVA is suitable for use as a gel matrix because its crosslinking degree is easily tuned by changes in annealing time. For example, a PVA matrix annealed at 200 °C for 10 min swells in water to twice the extent as does one annealed for 60 min. Similarly, in the presence of PAA (2.4×10^{-3} wt%), aragonite thin films with concentric ring patterns form on a PVA matrix annealed for 10 min, whereas films with dendritic patterns form on a PVA matrix annealed for 60 min.[23] Further increase in annealing time to 120 min results in formation of concentric calcite films.

$CaCO_3$ pattern generation in a spontaneous two-step growth process is also observed on a PVA gel matrix (Figure 4a).[24] A thinner PVA matrix treated at 180 °C for 30 min is used here.

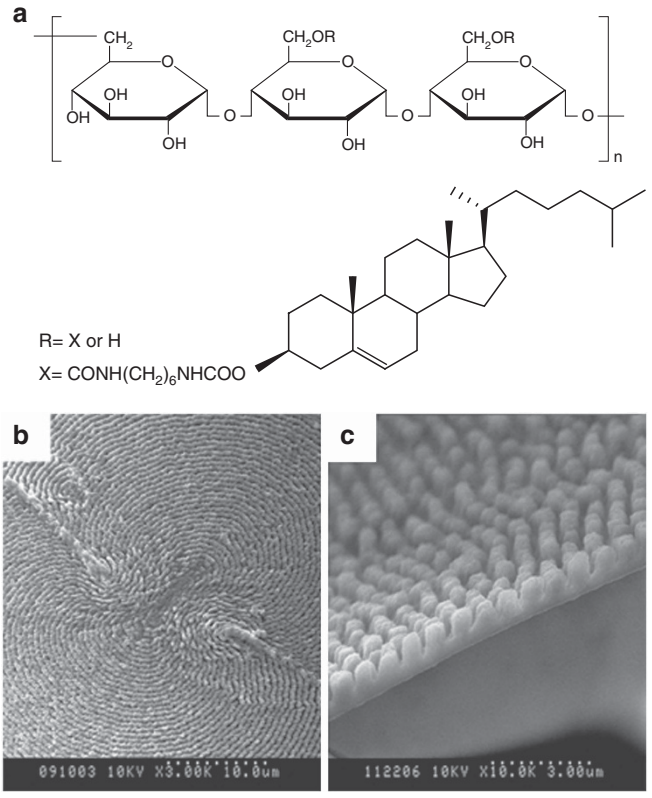

Figure 3 (**a**) Chemical structure of CHP. Other OH groups may also be substituted with X. (**b**, **c**) Scanning electron microscopy images of $CaCO_3$ thin films with surface-relief structures: (**b**) an area around the starting point of crystallization, (**c**) cross-sectional image. Adapted with permission from Sugawara *et al.*[21] Copyright (2003), Wiley-VCH.

In the first step, flat calcite thin film crystals grow on the PVA matrix, with their *c*-axis orientations changing periodically between perpendicular and parallel to one another (Figures 4b and c). In the second step, during prolonged incubation, needle-like crystals grow on the preformed thin film crystals (Figures 4d and e). The orientations of the *c*-axes of the needle-like crystals change periodically according to the *c*-axes of the underlying thin film crystals and results in formation of relief structures.

Sakamoto *et al.*[26] reported the site-controlled formation of patterned $CaCO_3$ films using a PVA derivative bearing photo-crosslinkable moieties as a gel matrix. The matrix is chemically crosslinked by irradiation with ultraviolet light. In the presence of PAA, a flat $CaCO_3$ film forms on a ultraviolet-irradiated matrix while a film with a relief structure forms on a nonirradiated matrix. Photopatterning of the matrix enables site-selective formation of $CaCO_3$ reliefs on the matrix with single-micrometer resolution.

Recently, Yamamoto *et al.*[27] have employed a three-dimensional gel matrix composed of liquid-crystalline chitin whiskers to obtain $CaCO_3$ hybrid materials. Three-dimensionally ordered $CaCO_3$ structures are formed in the cholesteric chitin gel, the arrangement of which resembles that in a crayfish exoskeleton.

Oriented $CaCO_3$ thin films

The crystallization system using insoluble and soluble macromolecules can be used to study the effect of biomineralization-involved protein on $CaCO_3$ crystallization.[28–30] The crayfish exoskeleton is a

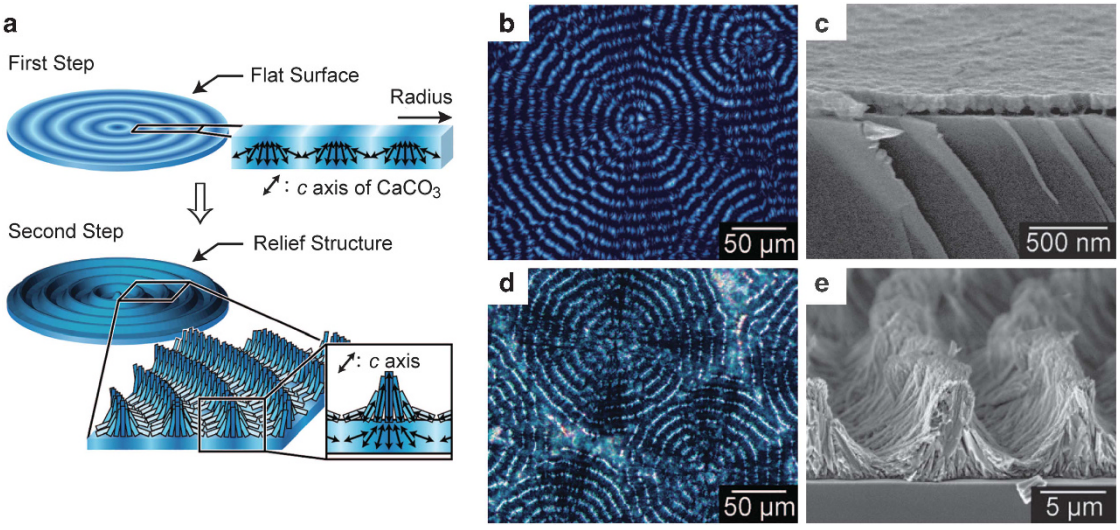

Figure 4 (**a**) Schematic illustration for the formation of three-dimensional relief structures. (**b**–**e**) $CaCO_3$ crystals grown on PVA matrices in the presence of PAA after incubation for (**b**, **c**) 8 h and (**d**, **e**) 16 h. (**b**, **d**) Polarizing optical microscopy image (top view); (**c**, **e**) Scanning electron microscopy images (side-view). Adapted with permission from Sakamoto *et al.*[24] Copyright (2009), American Chemical Society.

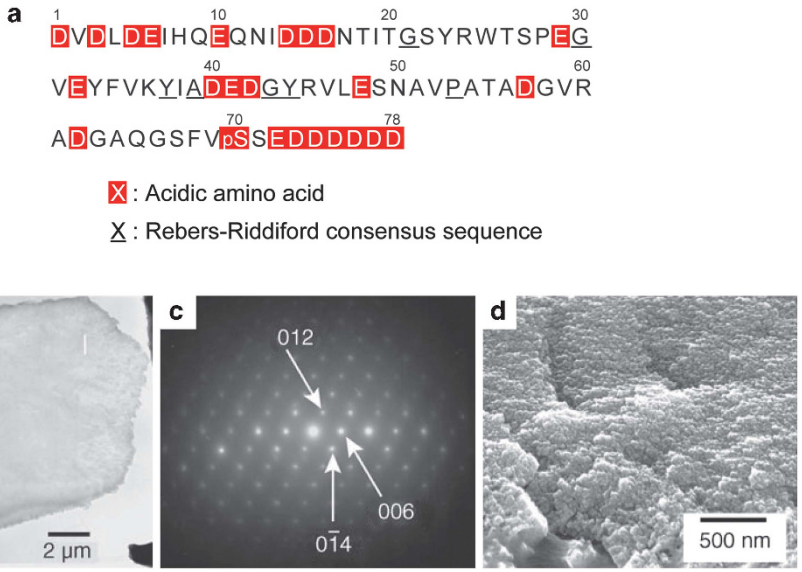

Figure 5 (**a**) Amino-acid sequence of CAP-1. pS, phosphoserine. (**b**) Transmission electron microscopy (TEM) image and (**c**) corresponding selected-area electron diffraction (SAED) image of the uniaxially oriented thin film crystal grown on a chitin matrix in the presence of CAP-1. (**d**) Scanning electron microscopy image of nanocrystals that consist of the thin film crystal. Adapted with permission from A Sugawara *et al.*[28] Copyright (2006), Wiley-VCH.

fascinating biomineral because of its remarkable mechanical properties. It consists mainly of chitin/protein microfibrils and $CaCO_3$ (calcite and ACC).[31] Inoue *et al.*[32] isolated a calcification-associated peptide-1 (CAP-1) from the exoskeleton of the crayfish *Procambarus clarkii*. CAP-1 is one of the soluble proteins present in the exoskeleton, and its amino-acid sequence has several unique features (Figure 5a). It is a highly acidic peptide that includes a 70th phosphoserine (pS) and a C-terminal Asp-repeat. It also has a Rebers–Riddiford consensus sequence, which is postulated to be involved in protein–chitin interaction. The calcium- and chitin-binding capability of the peptide has been verified experimentally and it indicates that CAP-1 is a mediating peptide between $CaCO_3$ and organic matrices in calcified tissues.[33]

Calcite thin films form in the presence of CAP-1 (3.0×10^{-3} wt%) on a chitin matrix.[28] The thin film is composed of nanocrystals with their *c*-axes oriented unidirectionally (Figures 5b–d). Real-time observation of $CaCO_3$ crystallization by polarizing optical microscopy drove us to speculate that the oriented film forms via amorphous-to-crystalline transformation. Comparable experiments using recombinant peptides and synthetic peptide fragments of CAP-1 reveal the role of each CAP-1 domain:[28,29] (1) rCAP-1, where the 70th pS is replaced with Ser, also gives oriented $CaCO_3$ thin films in which

primary particle size (that of the nanocrystals comprising the thin film) increases. pS has a stronger inhibitory effect on $CaCO_3$ crystallization than does Ser and thus might stabilize ACC. (2) Both CAP-1 derivatives lack 17 amino acids at its C-terminal, and the peptide fragment $pSSED_6$ gives bulk crystals of $CaCO_3$. Thus, both the Rebers–Riddiford consensus sequence and the C-terminal acidic domain are necessary to mediate association between $CaCO_3$ and chitin by inducing thin film crystallization of $CaCO_3$.

Suzuki *et al.*[30] recently identified an acidic matrix protein, Pif, in the pearl oyster *Pinctada fucata* that specifically binds to $CaCO_3$ aragonite crystals. Crystallization experiments were performed in the presence of a chitin matrix spin-coated onto a glass substrate. The protein fraction containing Pif induced formation of aragonite thin film crystals between the chitin matrix and glass substrate. The *c*-axis of the film was perpendicular to the film plane, as in a nacreous layer. Control proteins did not give such characteristic crystals. These results strongly support that Pif is involved in the biomineralization of nacre.

Nishimura *et al.*[34] demonstrated that orientation control of $CaCO_3$ can be accomplished by the combination of a designed solid matrix and a simple acidic polymer, instead of using complex proteins or peptides. Macroscopically oriented polymer–$CaCO_3$ hybrids were obtained by using liquid-crystalline chitin derivatives as a solid matrix and PAA as a soluble polymer additive. Aligned rod-like $CaCO_3$ were grown in the oriented matrix, which was prepared by stretching the liquid-crystalline film of the chitin derivative.

POLYMER NANOGEL–CALCIUM PHOSPHATE COMPOSITE NANOPARTICLES

Calcium phosphate, another important biomineral, is the major component of our bones and teeth. Materials based on calcium phosphate exhibit excellent biocompatibility and thus are of great interest as biomaterials. Polymer hydrogel nanoparticles (nanogels), another important class of materials, are effective for use in drug delivery systems. CHP (Figure 3a) spontaneously forms nanogels, about 30 nm in size, in water by the association of hydrophobic cholesteryl groups.[25] Biomedical applications of CHP nanogels have been investigated, especially applications involving their use as drug delivery system carriers of proteins, drugs and semiconductor nanocrystals.[35] However, CHP nanogels are not very stable, especially in the bloodstream, because of their physical crosslinking structure. It is expected that a hybrid composite formed from calcium phosphate and nanogel may exhibit improved stability and controlled-release properties.

Nanogel-templated mineralization was performed in dilute aqueous solution of calcium phosphate at room temperature.[36–38] A crystallizing solution of calcium phosphate was prepared by dissolving hydroxyapatite (HAp; $Ca_{10}(PO_4)_6(OH)_2$) powder in acidified water by bubbling CO_2 gas. A suspension of CHP nanogels was added to the solution. The final concentrations of nanogels and $[Ca^{2+}]$ were 0.5 mg ml^{-1} and 0.8 mM, respectively. Formation of calcium phosphate is driven by the increase in solution pH from 5.6 to 7.9 with a concurrent loss of CO_2 gas because calcium phosphate is more insoluble at higher pH.

Amorphous calcium phosphate (ACP) particles about 30 nm in size were obtained in the presence of CHP nanogel (whose particle size is about equivalent) (Figure 6a).[36] The calcium/phosphate (Ca/P) ratio in the ACP particles was 1.6, which is identical to that in the HAp starting solution. Aggregated ACP nanoparticles <20 nm in size formed in the presence of unmodified pullulan, which does not form nanogels because of its lack of hydrophobic groups (Figure 6b). No obvious precipitation was observed in the absence of additives. These

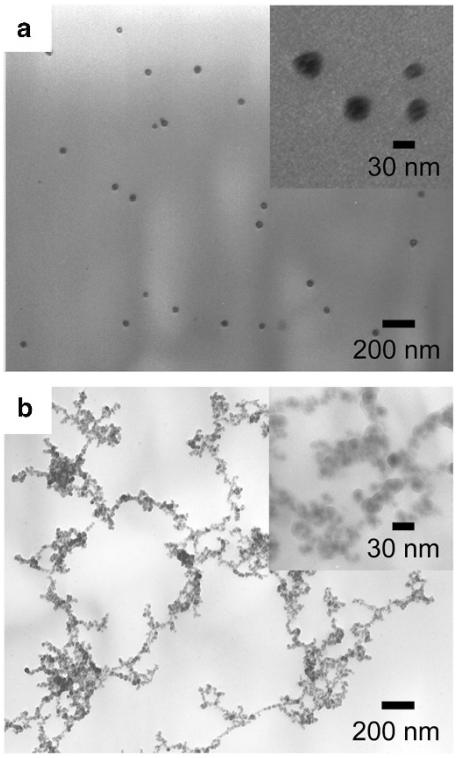

Figure 6 TEM images of calcium phosphate nanoparticles formed in the presence of (**a**) CHP nanogels and (**b**) pullulan. Insets show magnified images of the corresponding samples. Adapted with permission from Sugawara *et al.*[36] Copyright (2006), Wiley-VCH.

results indicate that CHP nanogels act as a scaffold for ACP formation. CHP–ACP hybrid nanoparticles are stable against aggregation or phase transformation in water for at least several months.

ACP composition can be controlled by the use of nanogels having anionic or cationic functional groups.[37] Accordingly, CHPs were modified with β-alanine and ethylenediamine, which have COOH and NH_2 groups, respectively. These groups are mostly negatively (COO^-) and positively (NH_3^+) charged under the present condition. ACP nanoparticles were also obtained by using those charged nanogels. The Ca/P ratios for the ACP nanoparticles are 2.9 for β-alanine-modified and 1.3 for ethylenediamine-modified nanogels, thus, suggesting that the ionic groups can interact with inorganic ions of opposite charges and accumulate them in the nanogels.

When the initial $[Ca^{2+}]$ was increased to >0.8 mM, HAp crystallized from solution. However, crystal size is difficult to control owing to heavy aggregation even in the presence of CHP nanogels or their ionic derivatives. The use of nanogels composed of cholesterol-bearing mannan (CHM), a branching polysaccharide containing phosphodiester bonds (Figure 7a), turns out to be effective for obtaining polymer–HAp hybrid nanoparticles of controlled size.[38] CHM formed self-assembled nanogels about 20 nm in size in water. In the presence of such CHM nanogels, ACP nanoparticles with a mean diameter of 19 nm formed just after the nanogel suspension and the crystallizing solution were mixed (Figure 7b). They transformed into HAp crystals within 24 h and further crystal growth then proceeded. Finally, needle-shaped HAp crystals about 85 nm in length were obtained (Figure 7c), which remained colloidally stable over several

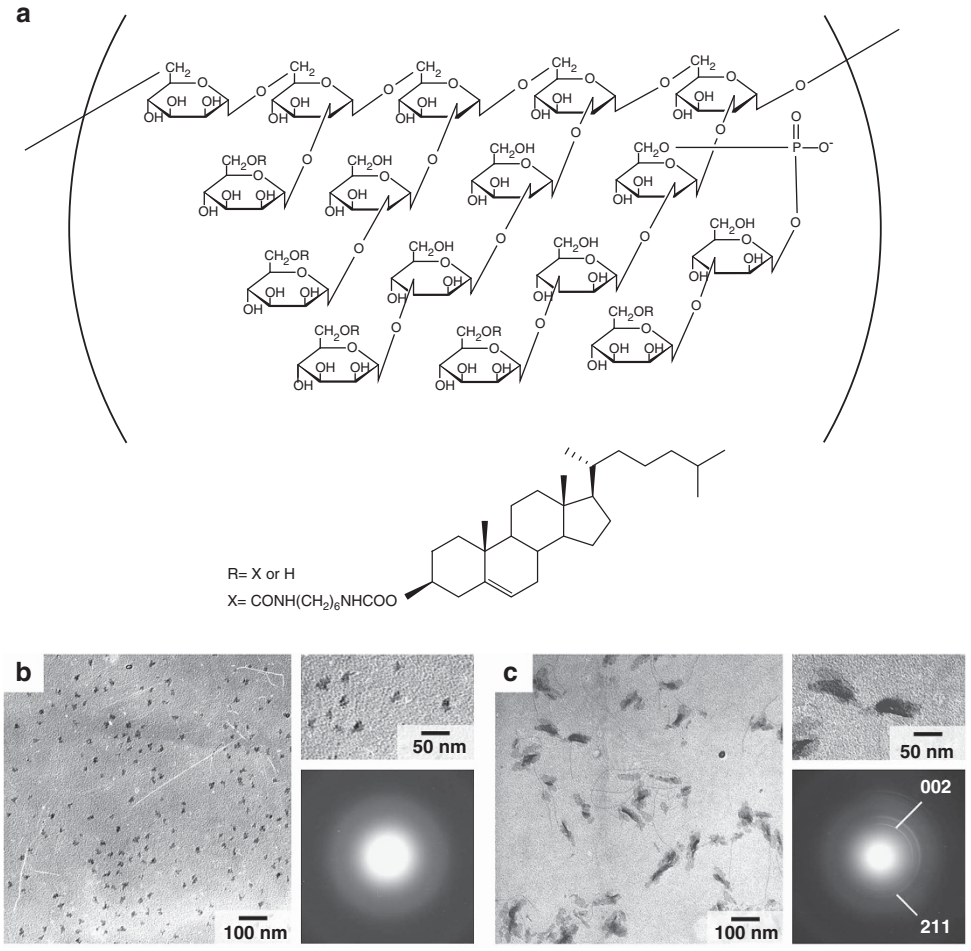

Figure 7 (**a**) Chemical structure of CHM. (**b**, **c**) TEM images and SAED patterns of calcium phosphates prepared in the presence of CHM nanogels at $[Ca^{2+}] = 2.0$ mM: (**b**) just after preparation (0 h) and (**c**) 24 h. Adapted with permission from Yamane *et al.*[38] Copyright (2009), SAGE Publications.

months. Hybrid formation between CHM and HAp was confirmed by addition of Concanavalin A (ConA), a lectin protein that binds to specific structures found in mannose sugars. If CHM polymer chains were to be exposed on the outer surfaces of hybrid nanoparticles, they would interact with ConA and aggregate in the suspension because ConA has four binding sites for mannose per molecule. The turbidity of the suspension started to increase because of the aggregation of HAp crystals after addition of ConA, which indicates that the HAp crystals were wholly or partly covered by the polysaccharide chains of the CHM nanogel. CHM nanogel may limit the size of the hybrid nanoparticles by interacting with growing HAp crystals as well as providing them with excellent colloidal stability.

SILICA NANOPARTICLES SELF-ASSEMBLED INTO CHAIN-LIKE STRUCTURES

Sophisticated nanostructures in biominerals are often fabricated via assembly of preformed building blocks. For example, curved rods of silica assemble into basket-like lorica.[39] Similarly, $CaCO_3$ nanoplates assemble into necklace-like structures in the early stage of coccolith formation.[40] Such a controlled assembly of colloidal particles that act as building units have recently attracted much attention in materials science.[41] It has been found that colloidal silica nanospheres (SNSs) assemble into one-dimensional (1D) chain-like structures in water with the aid of a block copolymer, as described below.[42]

Colloidal suspension of SNSs about 15 nm in size was prepared by the method reported by Yokoi *et al.*[43] This method uses a biphasic liquid system containing tetraethoxysilane, water and L-lysine as a catalyst to give monodisperse SNSs. SNSs are colloidally stable at around and above neutral pH because they are electrostatically repulsive (the isoelectric point of silica is pH 2–3). Block copolymer Pluronic F127 (BASF, Ludwigshafen, Germany) was used to mediate 1D assembly of SNSs.[42] F127 is a non-ionic triblock copolymer consisting of poly (ethylene oxide) and poly(propylene oxide) (PEO-*b*-PPO-*b*-PEO) with an average molecular weight of 12 600 and 70 wt% PEO content. F127 is known to adsorb onto silica surfaces via hydrogen bonding between the ether oxygen atoms of PEO and the silanol groups of silica.[44]

F127 was dissolved in the SNSs suspension ($F127/SiO_2 = 1$ (w/w)), the pH of the suspension was adjusted to 7.2–7.5, and the suspension was subjected to static incubation at 60 °C. A time-dependent turbidity profile of the suspension shows that turbidity increased gradually over 2 weeks, and the suspension eventually formed a weak gel (Figure 8a). Cryogenic transmission electron microscopy revealed that a 1D chain-like structure of SNSs formed in the liquid phase (Figure 8b). The number of connected SNSs increased with increasing incubation time.

The effect of F127 addition on a reaction system depends on its relative concentration. With sufficient amounts of F127 ($F127/SiO_2 = 0.8 \sim 2$), the SNSs self-assemble to form 1D chains. With a

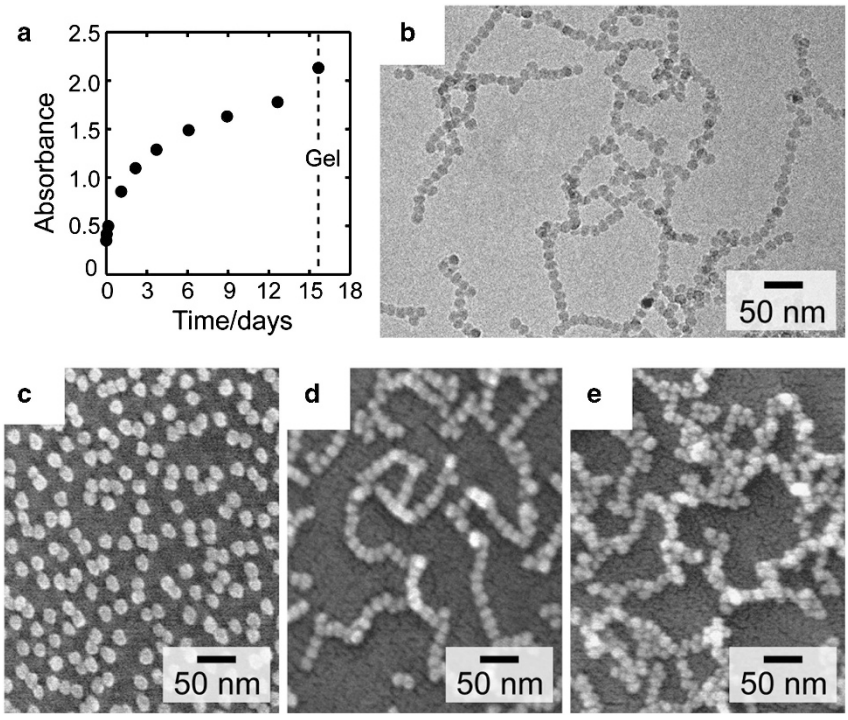

Figure 8 (**a**) Time-dependent turbidity profile of SNSs suspension containing F127 (pH 7.5) measured by ultraviolet–visible spectroscopy. The absorbance increases across the entire wavelength range of 300–800 nm. The representative data at 350 nm are shown here. (**b**) Cryo-TEM image of the frozen-hydrated sample at pH 7.2 after 8 days of incubation. (**c**–**e**) Scanning electron microscopy images of SNSs transferred to a Si substrate. These structures are formed in the presence of F127 at pH (**a**) 8.0, (**b**) 7.0 and (**c**) 6.0 after 7 days of incubation. Adapted with permission from Fukao *et al.*[42] Copyright (2009), American Chemical Society.

much smaller amount of F127 ($F127/SiO_2 = 0.1$), the SNSs immediately aggregate because of bridging flocculation, wherein a polymer adsorbs onto two or more particles simultaneously.

The mode of particle assembly is sensitive to the pH of the suspension. F127 was mixed with SNSs ($F127/SiO_2 = 1$) and incubated at 60 °C for 7 days under various pH conditions between 8.0 and 6.0. At pH 8.0, the SNSs remained dispersed (Figure 8c); at pH 7.5, 1D chains along with relatively unbranched straight structures were formed; at pH 7.0, bent chains with branches were formed (Figure 8d); and at pH 6.0, more disordered SNSs assemblies were formed (Figure 8e). This pH dependency may be explained by the reduction of electrostatic repulsion between SNSs. The charge density of SNSs decreases with decreasing pH because of the protonation of SiO^- groups. It seems that the delicate balance between electrostatic repulsion between SNSs and F127-mediated attractive interaction is important for 1D assembly of SNSs.

The origin of the observed anisotropic assembly remains a question to be explored. Au nanoparticles surrounded by layers of crosslinked poly(stylene-*block*-acrylic acid) reportedly form 1D chains in the liquid phase.[45] In this case, 1D chains form by the transition of micelles in the block copolymer from spherical to worm-like, which also occurs in the absence of Au nanoparticles. In the present system, however, formation of worm-like micelles in the absence of SNSs was not observed, thus suggesting that a synergistic effect of F127 and SNSs might contribute to 1D assembly. The elucidation of the mechanism of the anisotropic assembly of SNSs as well as the exploration of novel synthetic route of building blocks[46–48] is under progress.

CONCLUSION

Inspired by biomineralization, a variety of nanocomposite materials—including polymer–$CaCO_3$ thin films, polymer–calcium phosphate nanoparticles and SNS chains—were fabricated in mild aqueous systems. The nanostructured materials can be constructed spontaneously in one-pot processes via the controlled growth of inorganic crystals or the self-assembly of building blocks, which are mediated by macromolecules. Given that relatively simple macromolecules are sufficiently effective for composite formation, there is still plenty of room for creativity in these bio-inspired materials syntheses. I expect that this research area will eventually integrate with areas involving state-of-the-art functional polymers and inorganic materials, which will lead to the development of novel materials that overcome the limitations of biotic materials.

CONFLICT OF INTEREST

The author declares no conflict of interest.

ACKNOWLEDGEMENTS

I thank all co-workers for their great contributions reported in this review. I am deeply indebted to Professor Takashi Kato (The University of Tokyo), Professor Kazunari Akiyoshi (Kyoto University) and Professor Tatsuya Okubo (The University of Tokyo) for their continuous encouragement and constructive discussions. A part of this work was supported by a Grant-in-Aid for Scientific Research (No. 22107005) on the Innovative Areas: 'Fusion Materials' (Area no. 2206) from the Ministry of Education, Culture, Sports, Science and Technology (MEXT), Japan.

1 Mann, S. In: *Biomineralization–Principles and Concepts in Bioinorganic Materials Chemistry* (eds Compton, R. G., Davies, S. G. & Evans, J.) (Oxford University Press, New York, 2001).
2 Weiner, S. & Addadi, L. Design strategies in mineralized biological materials. *J. Mater. Chem.* **7,** 689–702 (1997).
3 Meldrum, F. C. & Cölfen, H. Controlling mineral morphologies and structures in biological and synthetic systems. *Chem. Rev.* **108,** 4332–4432 (2008).
4 Weiner, S., Traub, W. & Parker, S. B. Macromolecules in mollusc shells and their functions in biomineralization. *Phil. Trans. R. Soc. Lond. B* **304,** 425–434 (1984).
5 Weiner, S. & Wagner, H. D. The material bone: structure-mechanical function relations. *Annu. Rev. Mater. Sci.* **28,** 271–298 (1998).
6 Kato, T., Sugawara, A. & Hosoda, N. Calcium carbonate–organic hybrid materials. *Adv. Mater.* **14,** 869–877 (2002).
7 Oaki, Y., Adachi, R. & Imai, H. Self-organization of hollow-cone carbonate crystals through molecular control with an acid organic polymer. *Polym. J.* **44,** 612–619 (2012).
8 Sommerdijk, N. A. J. M. & de With, G. Biomimetic $CaCO_3$ mineralization using designer molecules and interfaces. *Chem. Rev.* **108,** 4499–4550 (2008).
9 Oaki, Y., Kotachi, A., Miura, T. & Imai, H. Bridged nanocrystals in biominerals and their biomimetics: classical yet modern crystal growth on the nanoscale. *Adv. Funct. Mater.* **16,** 1633–1639 (2006).
10 Kato, T. Polymer/calcium carbonate layered thin-film composites. *Adv. Mater.* **12,** 1543–1546 (2000).
11 Kato, T., Suzuki, T., Amamiya, T., Irie, T. & Komiyama, M. Effects of macromolecules on the crystallization of $CaCO_3$ the formation of organic/inorganic composites. *Supramol. Sci.* **5,** 411–415 (1998).
12 Kato, T. & Amamiya, T. A new approach to organic/inorganic composites. thin film coating of $CaCO_3$ on a chitin fiber in the presence of acid-rich macromolecules. *Chem. Lett.* **28,** 199–200 (1999).
13 Kato, T., Suzuki, T. & Irie, T. Layered thin-film composite consisting of polymers and calcium carbonate: A novel organic/inorganic material with an organized structure. *Chem. Lett.* **29,** 186–187 (2000).
14 Hosoda, N. & Kato, T. Thin-film formation of calcium carbonate crystals: effects of functional groups of matrix polymers. *Chem. Mater.* **13,** 688–693 (2001).
15 Sugawara, A., Oichi, A., Suzuki, H., Shigesato, Y., Kogure, T. & Kato, T. Assembled structures of nanocrystals in polymer/calcium carbonate thin-film composites formed by the cooperation of chitosan and poly(aspartate). *J. Polym. Sci. A, Polym. Chem.* **44,** 5153–5160 (2006).
16 Kitano, Y. The behavior of various inorganic ions in the separation of calcium carbonate from a bicarbonate solution. *Bull. Chem. Soc. Jpn* **35,** 1973–1980 (1962).
17 Falini, G., Gazzano, M. & Ripamonti, A. Crystallization of calcium carbonate in presence of magnesium and polyelectrolytes. *J. Cryst. Growth* **137,** 577–584 (1994).
18 Sugawara, A. & Kato, T. Aragonite $CaCO_3$ Thin-film formation by cooperation of Mg^{2+} and organic polymer matrices. *Chem. Commun.* **6,** 487–488 (2000).
19 Sugawara, A. & Kato, T. Calcium carbonate/polymer composites: polymorph control for aragonite. *Compos. Interfaces* **11,** 287–295 (2004).
20 Hosoda, N., Sugawara, A. & Kato, T. Template effect of crystalline poly(vinyl alcohol) for selective formation of aragonite and vaterite $CaCO_3$ thin films. *Macromolecules* **36,** 6449–6452 (2003).
21 Sugawara, A., Ishii, T. & Kato, T. Self-organized calcium carbonate with regular surface-relief structures. *Angew. Chem. Int. Ed.* **42,** 5299–5303 (2003).
22 Sakamoto, T., Oichi, A., Sugawara, A. & Kato, T. Self-organization of patterned $CaCO_3$/polymer composite films: tuning of their morphologies by the change of molecular weights of acidic polymers. *Chem. Lett.* **35,** 310–311 (2006).
23 Sakamoto, T., Oichi, A., Nishimura, T., Sugawara, A. & Kato, T. Calcium carbonate/polymer thin-film hybrids: induction of the formation of patterned aragonite crystals by thermal treatment of a polymer matrix. *Polym. J.* **41,** 522–523 (2009).
24 Sakamoto, T., Oichi, A., Oaki, Y., Nishimura, T., Sugawara, A. & Kato, T. Three-dimensional relief structures of $CaCO_3$ crystal assemblies formed by spontaneous two-step crystal growth on a polymer thin film. *Cryst. Growth Des.* **9,** 622–625 (2009).
25 Akiyoshi, K., Deguchi, S., Moriguchi, N., Yamaguchi, S. & Sunamoto, J. Self-aggregates of hydrophobized polysaccharides in water. formation and characteristics of nanoparticles. *Macromoleucles* **26,** 3062–3068 (1993).
26 Sakamoto, T., Nishimura, Y., Nishimura, T. & Kato, T. Photoimaging of self-organized $CaCO_3$/polymer hybrid films by formation of regular relief and flat surface morphologies. *Angew. Chem. Int. Ed.* **50,** 5856–5859 (2011).
27 Yamamoto, Y., Nishimura, T., Saito, T. & Kato, T. $CaCO_3$/chitin-whisker hybrids: formation of $CaCO_3$ crystals in chitin-based liquid-crystalline suspension. *Polym. J.* **42,** 583–586 (2010).
28 Sugawara, A., Nishimura, T., Yamamoto, Y., Inoue, H., Nagasawa, H. & Kato, T. Self-organization of oriented calcium carbonate/polymer composites: effects of a matrix peptide isolated from the exoskeleton of a crayfish. *Angew. Chem. Int. Ed.* **45,** 2876–2879 (2006).
29 Yamamoto, Y., Nishimura, T., Sugawara, A., Inoue, H., Nagasawa, H. & Kato, T. Effects of peptides on $CaCO_3$ crystallization: mineralization properties of an acidic peptide isolated from exoskeleton of crayfish and its derivatives. *Cryst. Growth Des.* **8,** 4062–4065 (2008).
30 Suzuki, M., Saruwatari, K., Kogure, T., Yamamoto, Y., Nishimura, T., Kato, T. & Nagasawa, H. An acidic matrix protein, Pif, is a key macromolecule for nacre formation. *Science* **325,** 1388–1390 (2009).
31 Travis, D. F. Structural features of mineralization from tissue to macromolecular levels of organization in the decapod crustacea. *Ann. N. Y. Acad. Sci.* **109,** 177–245 (1963).
32 Inoue, H., Ozaki, N. & Nagasawa, H. Purification and structural determination of a phosphorylated peptide with anti-calcification and chitin-binding activities in the exoskeleton of the crayfish, *Procambarus clarkii. Biosci. Biotechnol. Biochem.* **65,** 1840–1848 (2001).
33 Inoue, H., Ohira, T., Ozaki, N. & Nagasawa, H. A novel calcium-binding peptide from the cuticle of the crayfish, *Procambarus clarkii. Biochem. Biophys. Res. Commun.* **318,** 649–654 (2004).
34 Nishimura, T., Ito, T., Yamamoto, Y., Yoshio, M. & Kato, T. Macroscopically ordered polymer/$CaCO_3$ hybrids prepared by using a liquid-crystalline template. *Angew. Chem. Int. Ed.* **47,** 2800–2803 (2008).
35 Sasaki, Y. & Akiyoshi, K. Self-assembled nanogel engineering for advanced biomedical technology. *Chem. Lett.* **41,** 202–208 (2012).
36 Sugawara, A., Yamane, S. & Akiyoshi, K. Nanogel-templated mineralization: polymer-calcium phosphate hybrid nanomaterials. *Macromol. Rapid Commun.* **27,** 441–446 (2006).
37 Yamane, S., Sugawara, A., Sasaki, Y. & Akiyoshi, K. Nanogel–calcium phosphate hybrid nanoparticles with negative or positive charges for potential biomedical applications. *Bull. Chem. Soc. Jpn.* **82,** 416–418 (2009).
38 Yamane, S., Sugawara, A., Watanabe, A. & Akiyoshi, K. Hybrid nanoapatite by polysaccharide nanogel-templated mineralization. *J. Bioact. Compat. Polym.* **24,** 151–168 (2009).
39 Leadbeater, B. S. C. in *Biomineralization in Lower Plants and Animals* (eds Leadbeater, B. S. C. & Riding, R.) 345–359 (Oxford University Press, New York, 1986).
40 Westbroek, P., de Jong, E. W., van der Wal, P., Borman, A. H., de Vrind, J. P. M., Kok, D., de Bruijn, W. C. & Parker, S. B. Mechanism of calcification in the marine alga *Emiliania huxleyi. Phil. Trans. R. Soc. Lond. B* **304,** 435–444 (1984).
41 Li, F., Josephson, D. P. & Stein, A. Colloidal assembly: the road from particles to colloidal molecules and crystals. *Angew. Chem. Int. Ed.* **50,** 360–388 (2011).
42 Fukao, M., Sugawara, A., Shimojima, A., Fan, W., Arunagirinathan, M. A., Tsapatsis, M. & Okubo, T. One-dimensional assembly of silica nanospheres mediated by block copolymer in liquid phase. *J. Am. Chem. Soc.* **131,** 16344–16345 (2009).
43 Yokoi, T., Sakamoto, Y., Terasaki, O., Kubota, Y., Okubo, T. & Tatsumi, T. Periodic arrangement of silica nanospheres assisted by amino acids. *J. Am. Chem. Soc.* **128,** 13664–13665 (2006).
44 Malmsten, M., Linse, P. & Cosgrove, T. Adsorption of PEO-PPO-PEO block copolymers at silica. *Macromolecules* **25,** 2474–2481 (1992).
45 Kang, Y., Erickson, K. J. & Taton, T. A. Plasmonic nanoparticle chains via a morphological, sphere-to-string transition. *J. Am. Chem. Soc.* **127,** 13800–13801 (2005).
46 Wang, J., Sugawara, A., Shimojima, A. & Okubo, T. Preparation of anisotropic silica nanoparticles via controlled assembly of presynthesized spherical seeds. *Langmuir* **26,** 18491–18498 (2010).
47 Wang, J., Sugawara-Narutaki, A., Fukao, M., Yokoi, T., Shimojima, A. & Okubo, T. Two-phase synthesis of monodisperse silica nanospheres with amines or ammonia catalyst and their controlled self-assembly. *ACS Appl. Mater. Interfaces* **3,** 1538–1544 (2011).
48 Wang, J., Sugawara-Narutaki, A., Shimojima, A. & Okubo, T. Biphasic synthesis of colloidal mesoporous silica nanoparticles using primary amine catalysts. *J. Colloid Interface Sci.* **385,** 41–47 (2012).

Ayae Sugawara-Narutaki is currently an Assistant Professor of Department of Chemical System Engineering at The University of Tokyo. She was born in Miyagi, Japan, in 24th May 1976. She received her Doctorate Degree in Engineering from The University of Tokyo in 2004 under the supervision of Professor Takashi Kato. After her postdoctoral researches at Tokyo Medical and Dental University with Professor Kazunari Akiyoshi (2004–2007) and at California Institute of Technology with Professor David A Tirrell (2007–2008) as a JSPS postdoctoral fellow, she joined The University of Tokyo. Her research interest covers biopolymers, polymer-inorganic composites, bio-inspired materials, self-assembly and biomineralization. She received the Award for Encouragement of Research in Polymer Science from the Society of Polymer Science, Japan (2011).